GeroScience (2023) 45:1451–1469
https://doi.org/10.1007/s11357-023-00760-2

ORIGINAL ARTICLE

Effect of Nrf2 loss on senescence and cognition of tau-based P301S mice

Ruben Riordan · Wang Rong · Zhen Yu · Grace Ross · Juno Valerio · Jovita Dimas-Muñoz · Valeria Heredia · Kathy Magnusson · Veronica Galvan · Viviana I. Perez

Received: 5 December 2022 / Accepted: 20 February 2023 / Published online: 28 March 2023

Abstract Cellular senescence may contribute to chronic inflammation involved in the progression of age-related diseases such as Alzheimer's disease (AD), and its removal prevents cognitive impairment in a model of tauopathy. Nrf2, the major transcription factor for damage response pathways and regulators of inflammation, declines with age. Our previous work showed that silencing Nrf2 gives rise to premature senescence in cells and mice. Others have shown that Nrf2 ablation can exacerbate cognitive phenotypes of some AD models. In this study, we aimed to understand the relationship between Nrf2 elimination, senescence, and cognitive impairment in AD, by generating a mouse model expressing a mutant human tau transgene in an Nrf2 knockout (Nrf2KO) background. We assessed senescent cell burden and cognitive decline of P301S mice in the presence and absence of Nrf2. Lastly, we administered 4.5-month-long treatments with two senotherapeutic drugs to analyze their potential to prevent senescent cell burden and cognitive decline: the senolytic drugs dasatinib and quercetin (DQ) and the senomorphic drug rapamycin. Nrf2 loss accelerated the onset of hind-limb paralysis in P301S mice. At 8.5 months of age, P301S mice did not exhibit memory deficits, while P301S mice without Nrf2 were significantly impaired. However, markers of senescence were not elevated by Nrf2 ablation in any of tissues that we examined. Neither drug treatment improved cognitive performance, nor did it reduce expression of

Supplementary Information The online version contains supplementary material available at https://doi.org/10.1007/s11357-023-00760-2.

R. Riordan · W. Rong · Z. Yu · G. Ross · J. Valerio · J. Dimas-Muñoz · V. Heredia · V. I. Perez (✉)
Department of Biochemistry and Biophysics, Linus Pauling Institute, Oregon State University, 351 Linus Pauling Science Center, Corvallis, OR 97331, USA
e-mail: vpmcl@yahoo.com

R. Riordan · W. Rong · Z. Yu · G. Ross · J. Valerio · J. Dimas-Muñoz · V. Heredia · K. Magnusson · V. I. Perez
Linus Pauling Institute, Oregon State University, Corvallis, OR, USA

K. Magnusson
Department of Biomedical Sciences, Carlson College of Veterinary Medicine, Oregon State University, Corvallis, OR, USA

V. Galvan (✉)
Department of Biochemistry and Molecular Biology, Center for Geroscience and Healthy Brain Aging, University of Oklahoma Health Sciences Center, 740 Stanton L. Young Bvd BMSB 821, Oklahoma City, OK 73104, USA
e-mail: veronica-galvanhart@ouhsc.edu

V. Galvan
Oklahoma City VA Medical Center, US Department of Veterans Affairs, Oklahoma City, OK, USA

senescence markers in brains of P301S mice. Contrarily, rapamycin treatment at the doses used delayed spatial learning and led to a modest decrease in spatial memory. Taken together, our data suggests that the emergence of senescence may be causally associated with onset of cognitive decline in the P301S model, indicate that Nrf2 protects brain function in a model of AD through mechanisms that may include, but do not require the inhibition of senescence, and suggest possible limitations for DQ and rapamycin as therapies for AD.

Keywords Ageing · Tauopathy · Nrf2 · Alzheimer's disease · Rapamycin · DQ

Introduction

Alzheimer's disease (AD) is an age-driven neurodegenerative disease, characterized histopathologically by accumulation of amyloid-β plaques and tau neurofibrillary tangles in the brain [1, 2]. Aside from plaques and tangles, other brain changes such as brain inflammation, synaptic loss, brain atrophy, and metabolic dysregulation have been associated with AD [3]. As immunosurveillance mechanisms weaken or become overwhelmed by biological damage with age, chronic inflammation sets in and likely contributes to the development and progression of AD. Thus, understanding the underlying mechanisms aids in identifying biomarkers for early detection and therapeutics for slowing disease progression [4].

One potential source of chronic inflammation in all age-related diseases, including AD, is cellular senescence [5–7]. Cellular senescence is a cellular state characterized by an irreversible cell-cycle arrest and resistance to apoptosis that can be induced through a variety of stimuli, including telomere shortening, DNA damage, and mitotic oncogenes where cells secrete a panel of molecules deleterious to surrounding cells and tissue [8, 9]. Senescent cells have been shown to accumulate in a variety of tissues with age, including the sites of chronic diseases [10]. Research has shown that senescent cells are implicated in the development of AD [11–13] and aging pathologies [14] likely due to their secretion of inflammatory molecules. Senescence is identified by a set of biomarkers characterizing different aspects of the senescence program [5, 15], including increased levels of cell cycle arrest markers (such as p16 and p21), secretion of a variety of inflammatory cytokines and other factors referred to as the senescent associated secretory phenotype (SASP), and lysosomal expansion observed as senescence associated β-galactosidase (SAβ-gal) activity. The SASP has recently emerged as a potential biomarker for early detection of AD, though cellular senescence in the brain remains largely unexplored [16]. Recently, multiple groups have demonstrated that clearance of senescent cells delays the onset of age-related pathologies (such as physical frailty, loss of endurance, and cognitive decline) in aged mice as well as in tau-based AD mouse models [6, 11, 17].

There are a variety of senotherapeutic treatments designed to target cellular senescence, which can be classified as either senolytic or senomorphic drugs. Senolytics, such as the combination drug dasatinib and quercetin (DQ), clear senescent cells through the induction of apoptosis. Senomorphics, such as rapamycin, prevent accumulation of senescent cells by modulating senescence markers or suppressing the secretory phenotype [12, 18]. Long-term DQ treatment has been shown to alleviate senescence-related phenotypes in mice and clear senescent cells from the hippocampus of aged mice, reducing cognitive impairment [10]. However, the effects of DQ on brain senescence and cognition in AD mouse models remain largely unexplored. Rapamycin has been shown to extend lifespan and healthspan in various species including mice [19–21]. mTOR attenuation has positive impacts on a variety of age-related conditions such as metabolic diseases, immune disorders, neurodegenerative diseases, and the aging process in general [20–26]. Furthermore, rapamycin prevents senescent cell accumulation in different cell types and from multiple senescent inducers [27–30]. Studies indicate that rapamycin reduces AD-like pathology and improves cognition in the hAPP(J20) [31–33], P301S (PS19) [34], and viral vector-based P301L [35] mouse models of AD and tauopathy. Previous work in our lab showed that rapamycin can prevent, but not clear senescence in mouse embryonic fibroblasts as well as in the lung and adipose tissue of mice through the nuclear factor-erythroid factor 2-related factor 2 (Nrf2)-related pathway [27]. Similarly, other studies have also displayed that various senotherapeutic treatments including quercetin, ginsenoside Rg1,

and cordyceptin activate Nrf2 and result in increased expression of Nrf2 target genes [36–42].

Nrf2, referred to as the master regulator of the redox pathway, is also a key mediator of the beneficial effects of caloric restriction, and acts as an important part of a damage response pathway and regulator of inflammation [43]. Protein levels of Nrf2 are known to decline with age, giving rise to an increased vulnerability to biological damage [44, 45]. Translocation of Nrf2 to the nucleus in neurons and glial cells has been seen to be impaired the hippocampus of AD patients [46], and levels of Nrf2 and Nrf2 target genes are known to be further reduced in the brains of human and animal models of AD and related dementias, specifically in the neurons of the hippocampus [1, 46–48]. Furthermore, decreased Nrf2 levels have been observed in senescent fibroblasts and inhibition of Nrf2 promotes senescence in vitro [36, 38, 49]. Nrf2 knock out (Nrf2KO) mice exhibit cognitive decline, and seem to mimic the aging phenotype [50]. Similarly, breeding Nrf2KO mice with some Aβ mouse models of AD exacerbates the AD-like symptoms [51]. To date, no study has assessed how the loss of Nrf2 affects brain senescence in AD mouse models.

In our study, we aimed to define how loss of Nrf2 affects cognition and brain cellular senescence of transgenic MAPT^{P301S}PS19 (P301S) mice, which expresses high levels of P301S mutant human tau specifically in neurons. This model exhibits neurofibrillary tangle (NFT) deposition, neurodegeneration, and impaired cognitive function [6] as well as severe hind-limb paralysis and an inability to feed, resulting in death at an early age [52]. Cognition of Nrf2KO mice independent of P301S was not accessed in this study because previous studies showed that Nrf2KO mice in the C57BL/6 J genetic background did not exhibit spatial learning deficits as late as 12 months of age in the absence of AD-like mutations [53, 54]. To this end, we bred Nrf2KO mice with transgenic P301S mice to generate non-transgenic Nrf2 wildtype (WT), Nrf2KO, transgenic Nrf2 wildtype (P301SWT), and transgenic Nrf2KO (P301SKO) mice, and treated transgenic mice with either DQ, rapamycin, or vehicle from 4 to 8.5 months of age. All WT mice were treated with vehicle. We aimed to determine the potential of rapamycin and DQ treatment to prevent the exacerbation of cognitive decline resultant of Nrf2 ablation in P301S mice. Cognition was assessed through MWM testing at 8.5 months. Then, hippocampus, prefrontal cortex, whole brain, lung, and adipose tissue, along with astrocytes isolated from brain, were collected for analysis of senescent markers. We found that loss of Nrf2 greatly accelerated the development of hind-limb ataxia and paralysis in P301S mice from 13 to 10 months of age. P301SKO mice showed long-term memory impairment at 8.5 months of age, while P301SWT mice did not. However, loss of Nrf2 did not elevate levels of senescence in any tissue of P301S mice. Further, both high-dose rapamycin and DQ failed to improve cognitive performance or reduce senescent cell burden in the presence or absence of Nrf2. High-dose rapamycin instead seemed to impair cognition and potentially elevate levels of SAβ-gal activity.

Materials and methods

Mouse strains

This study received prior approval from Oregon State University Institutional Animal Care and Use Committee. MAPT^{P301S}PS19 (P301S) mice (JAX stock #008,169) [52] were purchased from The Jackson Laboratory and bred to C57BL/6 J for six generations. Nrf2KO mice (ICR background) were obtained from Dr. Masayuki and Yamamoto Kohoku, University of Japan, and then were backcrossed 10 times into the C57BL6/J genetic background. P301S mice were bred with Nrf2KO over multiple generations to generate non-transgenic Nrf2 WT, transgenic Nrf2 wildtype (P301SWT), and transgenic Nrf2KO (P301SKO) mice.

Animal treatment

For both the DQ and rapamycin experiments, mice were divided into five groups, each containing between 11 and 15 mice per sex. For the senolytic experiment, all WT mice received vehicle treatment, while P301SWT and P301SKO mice were randomly divided into drug and vehicle treatment groups. Treatment began at 4.5 months of age, continuing for 5 days a week, every other week until 8.5 months of age. Mice received dasatinib and quercetin by oral gavage at a dose of 5 and 50 mg kg^{-1}, respectively, diluted into vehicle or with the same volume of vehicle as controls [55–58]. For the rapamycin

experiment, all WT mice received vehicle treatment, while P301SWT and P301SKO mice were randomly divided into drug and vehicle treatment groups. Treatment began at 4.5 months of age, continuing every other day until 8.5 months of age. Mice received rapamycin by I.P. injection at a dose of 8 mg kg^{-1} diluted into vehicle or with the same volume of vehicle as controls [59]. This dose was chosen because it was used previously for short-intervention lifespan studies [59], as well as intervention for short-lived models of dilated cardiomyopathy, muscular dystrophy, and Leigh syndrome [26], a severe mitochondrial disease [60]. Although this dose is approximately fourfold higher than that used in lifespan studies [20–22] and in studies of rapamycin in mouse models of AD [25, 31–33, 61, 62], no toxic effects were described in any of the studies previously used. Mice were euthanized 48 h after the last dose of rapamycin, DQ, or vehicle, and a thorough necropsy was performed. Tissues were snap frozen in liquid nitrogen, then stored at − 80 °C for subsequent molecular work.

To determine onset of hind-limb ataxia, cohorts of WT ($n=10$), P301SWT ($n=11$), P301SKO ($n=11$), and Nrf2KO ($n=4$) mice were observed twice a week for evidence of weight loss and hind-limb clamping and the age of phenotypic onset was recorded. The data were plotted as a survival curve using the GraphPad Prism software and analyzed by log-rank test (Mantel-Cox test) comparing the P301SWT and P301SKO groups.

Morris water maze

Male and female P301S (PS19) and P301S X Nrf2KO mice at 8.5 months of age were tested in the Morris water maze (MWM) task, including acclimation (2 days); spatial memory testing, including 16 reference hidden trials or place trials, and a naive probe (ran without knowledge of platform location) and other probes at the beginning of every other day (4 days), reversal training (1 day), and visible (control) trials (1 day) as previously described [63]. Performance on the spatial and cued version of the MWM task was analyzed using the Any-maze software. Performance was measured as the corrected integrated path length (CIPL) [64, 65] for spatial learning and reversal trials. CIPL is a proximity score which takes the sum of the mouse's distances from the platform, corrected for the mouse's speed and initial distance from the platform [66]. Proximity scores such as CIPL have been found to be more reliable than latency or distance swam, as they avoid the variability in results introduced by differences in swimming speed and release locations [63]. Mean distance from the former platform location was used as a measure of spatial memory on probe trials. Performing probes at multiple points throughout training allows us to see a progression of memory formation, although it can negatively impact learning. Animals may not show any differences in probe trials after training, but may show it early on [63]. $N=11–14$ mice per group. Analyses were performed with repeated measures ANOVA (Fishers LSD post hoc tests were performed as indicated when main effects of place trial or treatment/genotype were observed) using Prism 6 (GraphPad, San Diego, CA, USA).

RT-qPCR analysis

mRNA was extracted using the RNeasy kit (Qiagen, Valencia, CA, USA). RNA was reverse-transcribed to cDNA using the SuperScript® IV FirstStrand Synthesis SuperMix following the manufacturer's instructions (Invitrogen). Target mRNA levels were measured by qPCR and normalized to beta actin (actb). Amounts of specific mRNA were quantified by determining the point at which fluorescence accumulation entered the exponential phase (Ct), and the Ct ratio of the target gene to actb was calculated for each sample. Ct ratios were further normalized to average WT expression. Information for qPCR primers is listed in Supplementary Table 1.

Western blotting

Brain tissue was homogenized in RIPA buffer supplemented with protease and protein phosphatase inhibitors (Calbiochem, La Jolla, CA) and subjected to SDS-PAGE followed by transferring to PVDF membranes (Millipore, Billerica, MA, USA). Membranes were incubated with antibodies specific for phosphor-tau (Ser 199, Ser 202), tau monoclonal antibody (Tau-5) (Thermo Fisher Scientific, Waltham, MA), and actin (MP Biomedicals, Solon, OH). The intensity of the bands was quantified by densitometry using the Imagelab software (Bio-rad, Hercules, CA).

Saβ-gal staining

SA-βgal staining was performed on coronal cryosections of hemibrains using the SPiDER-βgal kit (Dojindo Molecular Technologies, Rockville, MD, USA). Briefly, brain sections in groups of 3 were fixed onto slides with 4% paraformaldehyde, incubated with 80 µl of SPiDER-βgal working solution at 37 °C for 2.5 h, washed 3 times with PBS, then incubated with 4′,6-diamidino-2-phenylindole (DAPI), a fluorescent stain that binds tightly to adenine–thymine-rich regions of DNA at 4 °C overnight, and imaged (excitation: 488 nm; emission: 500–600 nm) using a Keyence fluorescence microscope.

Statistical analysis

QPCR and western blot data were analyzed using Prism 6 (GraphPad, San Diego, CA, USA). Significance of differences between experimental group means were defined using one-way ANOVA. Fisher's LSD tests were performed to ascertain differences between genotype/treatment means, and $p < 0.05$ was considered significant and reported as indicated in the legends to the figures.

Results

Nrf2 loss accelerated development of hind-limb paralysis in P301S mice

P301S mice express high levels of mutant human tau (hTau), roughly fivefold higher than endogenous mouse tau, resulting in rapidly lethal, early onset disease that is characterized by a severe hind-limb dystonia, paralysis, an inability to feed, and death at 9 months of age [52]. We observed a cohort of 10–12 animals, WT, P301SWT, P301SKO, and Nrf2KO mice over a period of 15 months after birth to generate a survival curve based on the onset of hind-limb paralysis (Fig. 1). Over the 15-month period, P301SKO mice developed hind-limb atrophy between 8.5 and 11 months of age, with 50% animals euthanized by 10 months of age. This was compared to P301SWT mice that developed hind-limb atrophy between 10.5 and 15 months of age, with 50% of the group euthanized by 13 months of age (Fig. 1).

No Nrf2KO mice and only one WT mouse were euthanized over the 15-month period. Only 4 Nrf2KO mice were observed for this study; however, mice of this genotype do not display hind-limb dysfunction at least until 20 months of age in other studies [67]. These results indicate that hind-limb ataxia was delayed in P301SWT mice compared to previously reported studies, and that loss of Nrf2 significantly accelerated the hind-limb atrophy in the P301SKO mice compared to the P301SWT group.

Nrf2 loss did not increase pTau levels in P301S brain

Elevated levels of tau and phosphorylated tau (pTau) in the spinal cord of P301S mice result in severe hind-limb ataxia [52], which is accelerated by loss of Nrf2. We analyzed the effect of Nrf2 ablation on tau and pTau levels in brains of P301S mice to determine whether acceleration of hindlimb ataxia correlates with increased pTau burden. Western blot analysis of P301S mouse brains showed a roughly 12-fold increase in tau levels and fourfold increase of pTau levels compared to WT controls. However, loss of Nrf2 did not increase either tau or pTau in P301SKO mice compared to the P301SWT group (Fig. 2).

Loss of Nrf2 accelerated long term memory decline of P301S mice

Our next goal was to determine if loss of Nrf2 worsens the cognitive decline observed in the P301S model. While it is common to measure senescence and cognition by MWM at 6 months of age in this model, our previous studies (Dorigatti et al. 2021) showed that in our hands, P301S did not exhibit senescence or cognitive decline at 6–7 months of age but developed senescence at 10 months of age [15]. Given that P301SKO mice begin developing hind-limb ataxia at 8.5 months of age, we judged 8.5 months to be the best age to measure senescence and cognition.

To assess spatial learning and memory and cognitive flexibility, we used the MWM on WT, P301SWT, and P301SKO mice at 8.5 months of age as described [63]. We found significant main effects of genotype and place trial in the MWM tasks (Supplementary Table 2). There was a main effect of place trial in the

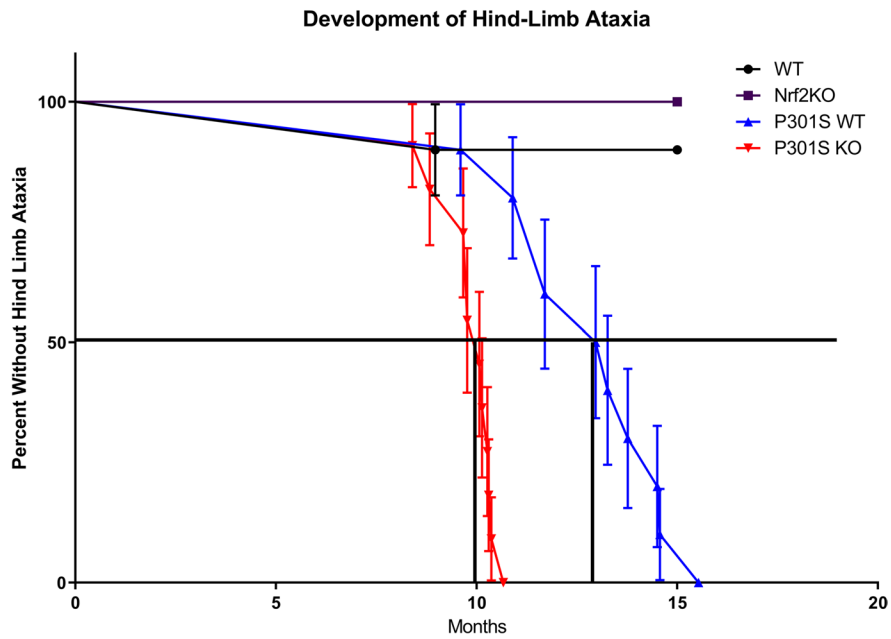

Fig. 1 Loss of Nrf2 accelerated the development of hind limb ataxia in P301S mice. Hind-limb clamping was observed and recorded weekly up to 8 months of age, and then monitored every other day up to 15 months of age. The purple line with squares represents Nrf2KO mice, the black line with circles represents WT mice, the blue line with triangles represents P301SWT mice, and the red line with triangles represents P301SKO mice. Each point represents death or the time at which hind-limb phenotype appeared, requiring mice to be euthanized. P301SKO mice developed hind limb ataxia at 10 months of age, which was significantly earlier than P301SWT mice at 13 months of age (log rank Mantel Cox test, $p < 0.0001$ for difference between P301SWT and P301SKO curves). Nrf2KO and WT mice largely did not experience the hind-limb phenotype, with 100 and 90% surviving past 15 months of age respectively. P301SKO $n = 11$, P301SWT $n = 10$, WT $n = 10$, Nrf2KO $n = 4$

spatial learning task for both male ($p < 0.0001$) and female mice ($p = 0.0138$). With data collapsed across genotype, both sexes showed lower CIPL measurements in the last trials as compared to the first ($p < 0.0001$).

There was a significant main effect of genotype on CIPL scores for spatial learning in female mice ($p < 0.001$; Supplementary Table 2): P301SKO mice had significantly higher CIPL scores on the spatial learning trials than WT mice ($p = 0.0484$), while P301SWT mice did not differ from WT ($p = 0.3485$; Fig. 3A–B). There was no significant main effect of genotype in the spatial learning task for males ($p = 0.1506$; Supplementary Table 2; Fig. 3C–D).

Probe trials were run at the beginning, middle, and end of the spatial learning process in which the platform was removed to test memory of the platform location. For female mice, there was no significant main effect of genotype in the probe trials ($p = 0.6763$; Supplementary Table 2; Fig. 3E–F). Males showed a trend for main effect of genotype on mean distance scores for probe trials ($p = 0.0562$; Supplementary Table 2): P301SKO mice had significantly higher mean distance scores on probe trials than WT mice ($p = 0.0184$), while P301SWT mice did not differ from WT ($p = 0.1262$; Fig. 3G–H).

To test cognitive flexibility, the platform location was moved, and mice were given four learning trials to learn the new platform location followed by a probe for the new and old platform locations. Among males, there was no significant main effect of genotype for reversal trials or the probe for new or old platform location ($p = 0.8179$–0.1726; Supplementary Table 2; Fig. 3I–J). There was a significant main effect of genotype on CIPL scores for female mice on reversal trials ($p = 0.0003$; Supplementary Table 2): Neither P301SWT nor P301SKO mice had significantly different CIPL scores than WT ($p = 0.1154$–0.0896; Fig. 3K–L).

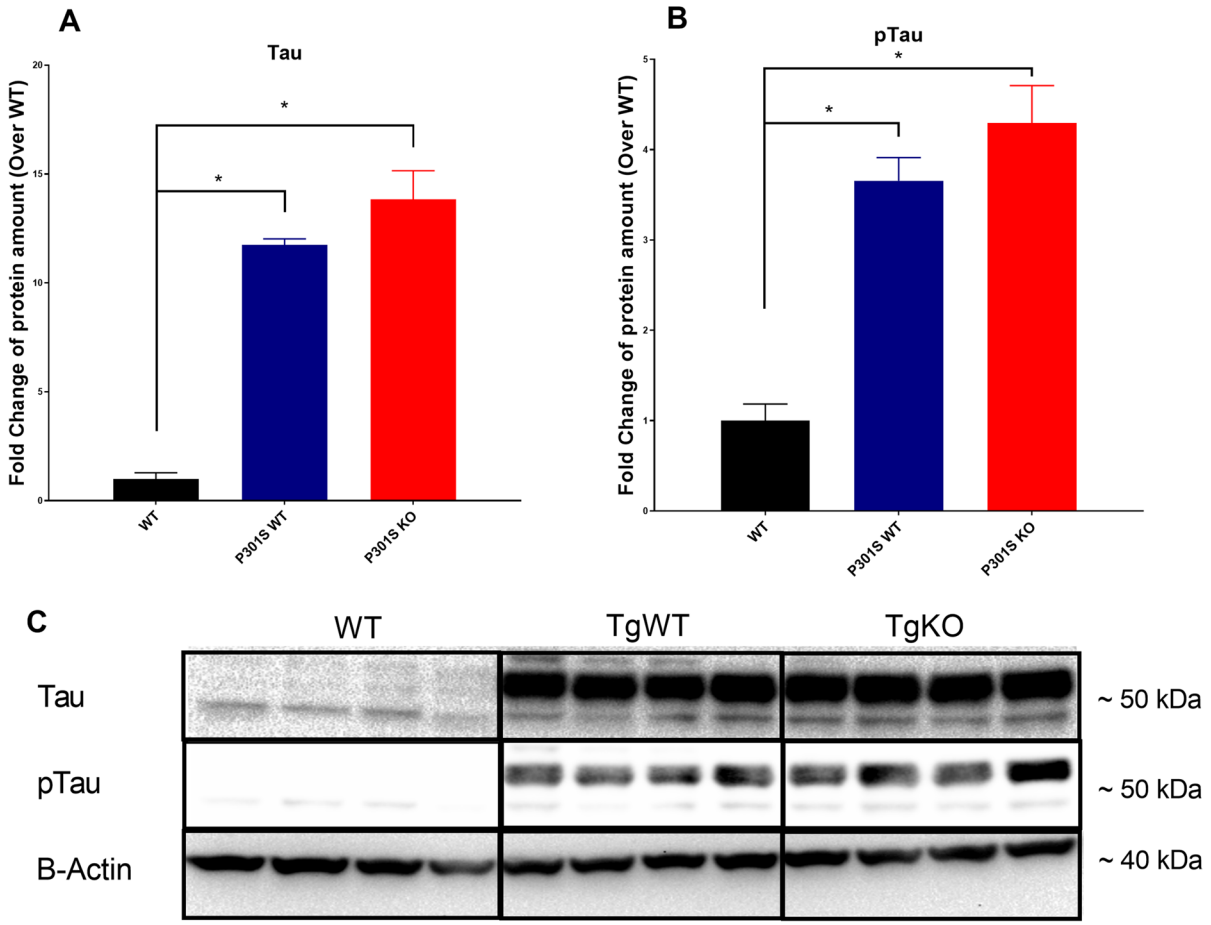

Fig. 2 Nrf2 ablation did not elevate brain levels of tau or ptau. Western blot analysis of tau (**A**) and ptau (**B**) protein expression in mouse brains at 8.5 months of age using anti-Tau monoclonal antibody (Tau-5) and anti-phosphoTau (Ser 199, Ser 202) antibody, normalized first to β-actin, and then WT expression. Representative western blot, Tau and pTau appear ~ 50–55 kDA, and β-actin appears at ~ 37–40 kDA (**C**). *$p < 0.05$ for differences between genotypes, one-way ANOVA with multiple comparisons, data = mean ± SEM)

Our data showed no main effect of genotype on CIPL scores for cued trials of either sex, indicating no visual deficiency ($p = 0.1674$–0.1253; Supplementary Table 2; Supplementary Fig. 2).

Loss of Nrf2 did not elevate levels of hippocampal senescence

In previous studies, the elimination of Nrf2 resulted in increased cellular senescence in vitro and in vivo [27]. To define the effect of Nrf2 loss on the accumulation of senescent cells in the hippocampus of P301S mice, we performed QPCR analysis on cell cycle arrest markers and common SASP factors from flash frozen hippocampus tissue collected from 8.5-month-old WT, P301SWT, and P301SKO mice, as well as SAβ-gal staining on hippocampus-containing brain cryo-sections from the same groups.

QPCR analysis of hippocampal tissue showed significant main effects of genotype for expression of SASP factors (F (2, 205) = 9.090; $p = 0.0002$) and cell cycle arrest markers (F (2, 65) = 7.283; $p = 0.0014$): P301SWT and P301SKO mice had significantly elevated levels of IL1-α, IL1-β, and p16 ($p = 0.0288$–< 0.0001) compared to WT mice. P301SWT and P301SKO mice also showed trends to elevations in ICAM1 and p21 expression ($p = 0.0669$–0.0611) compared to WT mice. However, P301SKO expression

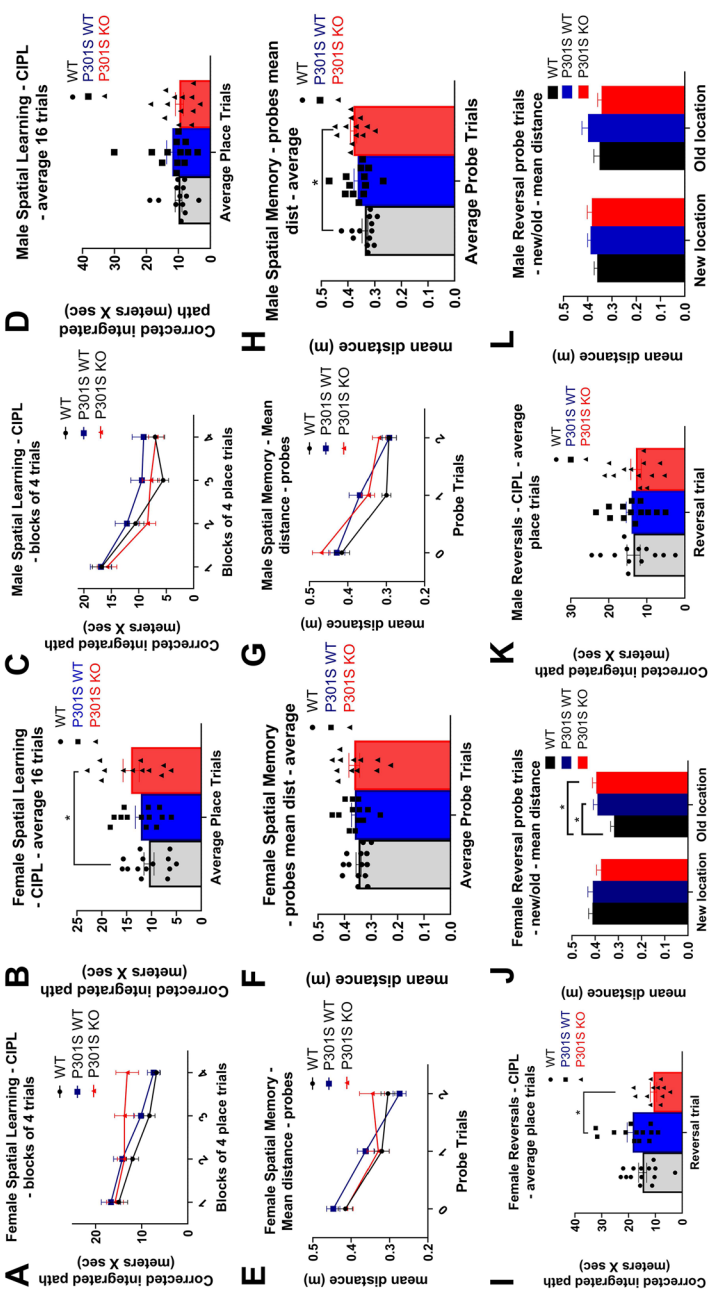

Fig. 3 Nrf2 elimination accelerated long-term memory decline in P301S mice. Analysis of MWM data for spatial learning, spatial memory, and cognitive flexibility for female and male WT (black lines and bars with circles), P301SWT (blue lines and bars with squares), and P301SKO (red lines and bars with triangles) mice at 8.5 months of age. Spatial learning ability of females and males reported as corrected integrated pathlength (CIPL), with higher values indicating worse performance. Female P301SKO mice had significantly higher CIPL scores than WT mice ($p = 0.0484$). Memory of platform location measured by mean distance from former platform location. Male P301SKO mice had significantly higher mean distance scores than WT mice ($p = 0.0184$). Cognitive flexibility determined by reversal place trials and new/old platform location probes ($n = 11$–14 per group, $^*p < 0.05$ for differences between genotypes defined by Fishers LSD post hoc test on a significant effect of genotype, ANOVA, data = mean ± SEM)

of all SASP factors and cell cycle arrest markers was similar to P301SWT mice ($p=0.998$–0.7785; Fig. 4A–B). This analysis was repeated in isolated brain astrocytes as well as in whole prefrontal cortex and in adipose tissue, yielding no significant increases of senescence markers in P301S mice regardless of Nrf2 status (Supplementary Fig. 1 a-j).

SAβ-gal staining showed no increase in β-gal activity in hippocampi of P301SWT or P301SKO mice compared to WT mice. Similarly, β-gal activity was similar for P301SWT mice compared to P301SKO (Fig. 4C).

Due to the lack of senescent cell accumulation, we searched for evidence of brain inflammation through expression of GFAP to indicate astrocyte activation. QPCR analysis showed a genotype effect of GFAP expression for the hippocampus (F (4, 16) = 3.567; $p=0.0291$): P301SWT ($p=0.0113$) and P301SKO ($p=0.0056$) mice expressed higher levels of GFAP than WT mice. However, P301SKO mice showed similar levels of GFAP to P301SWT ($p=$tHi0.7537; Supplementary Fig. 1 k-l).

Effect of senotherapeutic treatment on cognition

Previously, we showed that Nrf2KO mice exhibit increased levels of cellular senescence in adipose tissue and that rapamycin treatment mitigated levels of SASP expression [27]. As elimination of Nrf2 accelerated the cognitive decline of our P301S mice, we

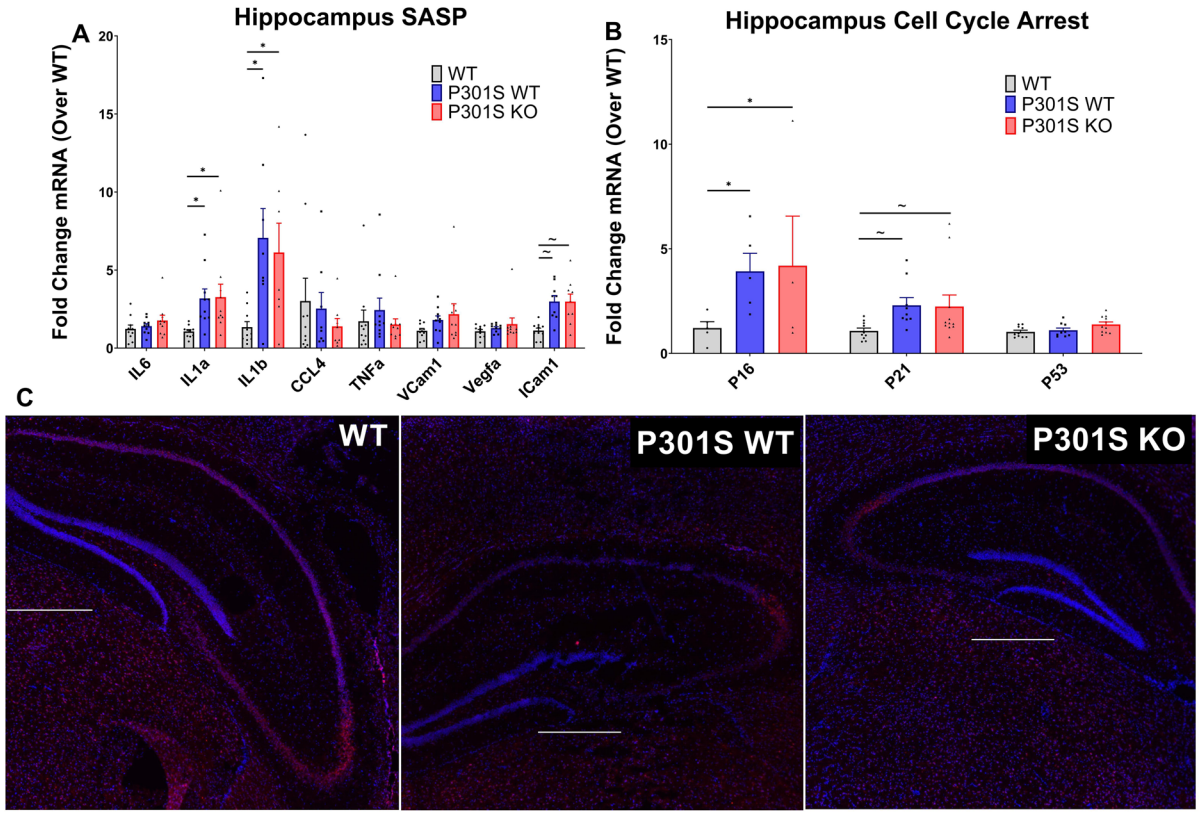

Fig. 4 Nrf2 loss did not exacerbate senescent cell burden in the hippocampus of P301S mice. Senescent cell burden was determined by analysis of 3 biomarkers: SASP, cell cycle arrest, and SAβ-gal activity. qPCR analysis of SASP (**A**) and cell cycle arrest markers (**B**) mRNA expression in hippocampus tissue of WT (white bars), P301SWT (gray bars), and P301SKO (black bars) mice at 8.5 months of age. P301SWT and P301SKO mice had significantly elevated levels of IL1-α, IL1-β, and p16 ($p=0.0288$–<0.0001) and positive trends for ICAM1 and p21 ($p=0.0669$–0.0611) compared to WT mice. Analysis of Saβ-gal activity (**C**), indicated by red fluorescence (total cell number, blue fluorescence), in brain cryo-sections from WT, P301SWT, or P301SKO mice (scale bar = 500 µm. $*p<0.05, \sim p<0.07$ for differences between genotypes, one-way ANOVA with multiple comparisons using Fishers LSD post hoc test, $n=8$–11 per group at 8.5 months of age, data = means ± SEM)

aimed to determine the ability of the senotherapeutic treatments, DQ and rapamycin, to prevent the impact of Nrf2 loss on cognition by MWM. For both therapeutics, either drug or vehicle treatment began at 4.5 months of age until completion of MWM testing at 8.5 months of age.

We found no significant main effects of genotype/treatment for spatial learning trials or long-term memory probes of DQ treated mice ($p = 0.1418$–0.1144; Supplementary Table 2; Fig. 5A–D).

For rapamycin treatment, we found a main effect of genotype/treatment for CIPL scores of spatial learning trials ($p = 0.0001$; Supplementary Table 2): Rapamycin treated P301SWT mice had significantly higher CIPL scores than vehicle treated WT ($p = 0.0065$) and P301SWT mice ($p = 0.0442$; Fig. 6A–B). There was also a significant main effect of genotype/treatment for mean distance scores on spatial memory probes for rapamycin treated mice ($p < 0.0001$; Supplementary Table 2): Rapamycin treated P301SWT mice had significantly higher mean distance scores than vehicle treated WT ($p = 0.0002$) and P301SWT mice ($p = 0.0366$). Rapamycin treated P301SKO mice had significantly higher mean distance scores than vehicle treated WT mice ($p = 0.0414$), while vehicle treated P301SKO mice did not differ from WT ($p = 0.1563$; Fig. 6C–D).

Effect of senotherapeutic treatment on brain senescence

Hippocampal QPCR analysis of P301S mice treated with DQ showed a significant main effect of genotype/treatment for SASP (F (4, 338) = 7.033; $p < 0.001$)

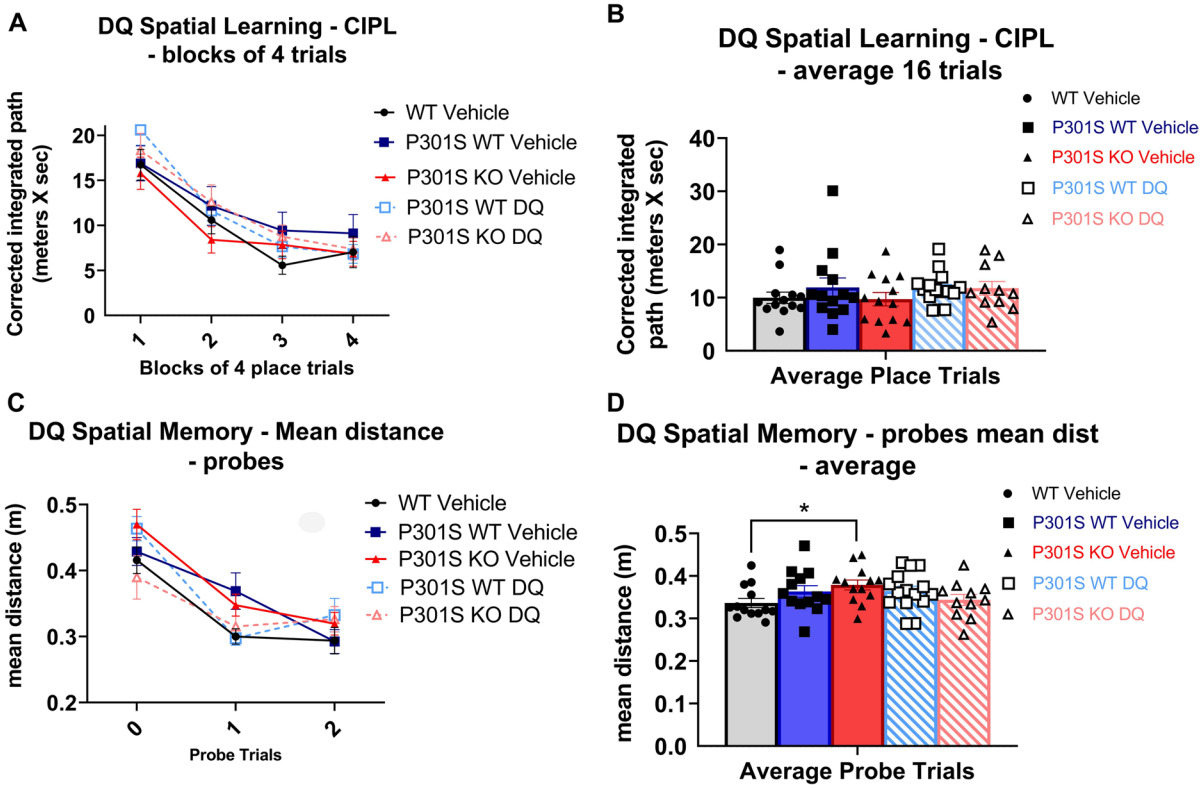

Fig. 5 DQ treatment did not improve cognitive performance in P301S mice. MWM analysis of long-term memory of DQ treated mice (WT vehicle = black lines and bars with circles, P301SWT vehicle = blue lines and bars with squares, P301SKO vehicle = red lines and bars with triangles, P301SWT DQ = striped blue with squares, P301SKO DQ = striped red with triangles). Spatial learning trials of DQ and vehicle treated mice shown in blocks of four and average of 16 trials. Long term memory probes of DQ and vehicle treated mice shown in individual probes and average of 3 probes ($n = 11$–14 per group, $^*p < 0.05$ for differences between genotypes or treatment defined by Fishers LSD post hoc test on a significant effect of genotype, ANOVA, data = mean ± SEM)

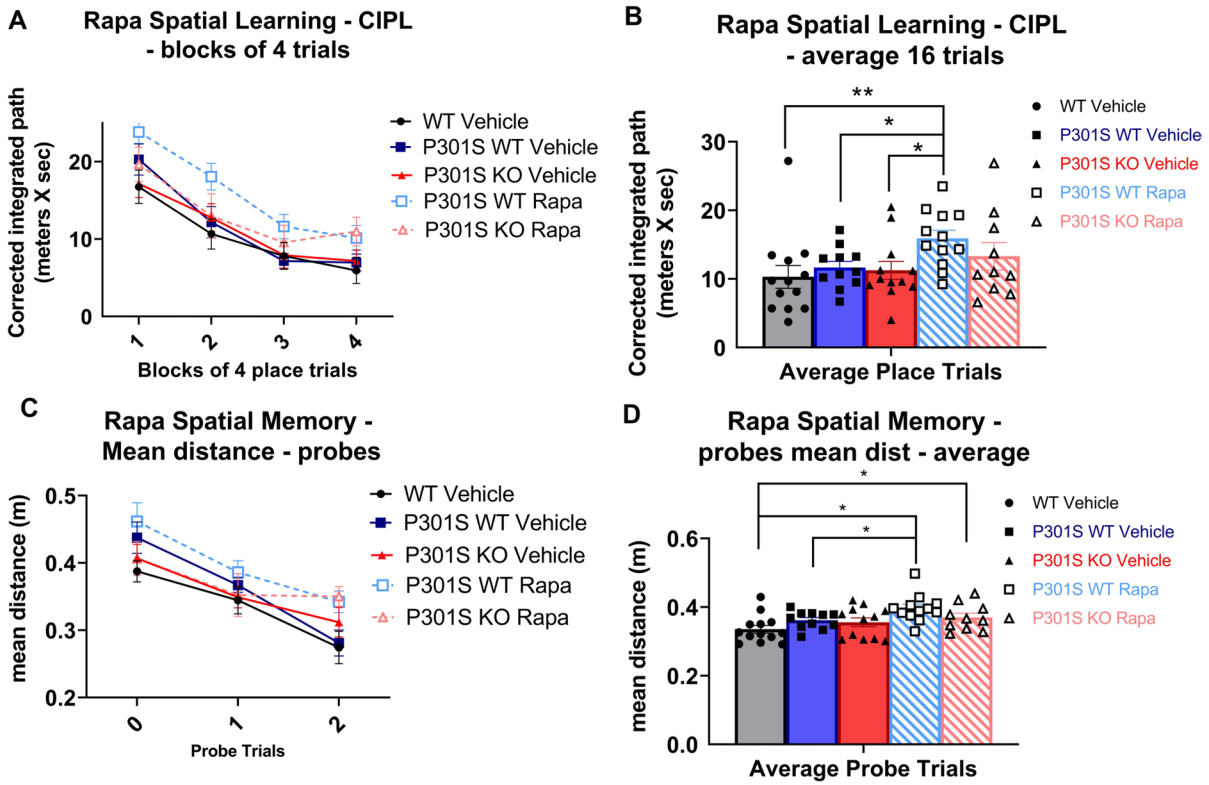

Fig. 6 Rapamycin treatment impaired cognition in P301S mice. MWM analysis of spatial learning and memory of rapamycin treated mice (WT vehicle = black lines and bars with circles, P301SWT vehicle = blue lines and bars with squares, P301SKO vehicle = red lines and bars with triangles, P301SWT rapamycin = striped blue with squares, P301SKO rapamycin = striped red with triangles). Spatial learning trials of rapamycin and vehicle treated mice shown in blocks of four and average of 16 trials. Rapamycin treated P301SWT mice had significantly higher CIPL scores than vehicle treated WT ($p = 0.0065$) and P301SWT mice ($p = 0.0442$). Spatial memory probes of rapamycin and vehicle treated mice shown in individual probes and average of 3 probes. Rapamycin treated P301SWT mice showed significantly higher mean distance scores than vehicle treated WT ($p = 0.0002$) and P301SWT mice ($p = 0.0366$). Rapamycin treated P301SKO mice had significantly higher mean distance scores than vehicle treated WT mice ($p = 0.0414$) ($n = 11$–14 per group, $^*p < 0.05$ for differences between genotypes or treatment defined by Fishers LSD post hoc test on a significant effect of genotype, ANOVA, data = mean ± SEM)

and cell cycle arrest markers (F (4, 104) = 4.087; $p = 0.0041$): DQ treated P301SWT and P301SKO mice expressed similar levels of SASP factors and cell cycle arrest markers compared to respective vehicle treated mice ($p = 0.8052$–0.0953; Fig. 7A–B), except for IL1β, which was reduced in DQ treated P301SKO mice compared to vehicle treated P301SKO mice ($p < 0.0001$). SAβ-gal staining on brain cryosections of DQ treated P301S mice showed no change in β-gal activity compared to vehicle treated transgenic mice, independent of Nrf2 status (Fig. 7C).

Hippocampal QPCR of transgenic mice treated with rapamycin showed a significant main effect of expression for SASP (F (4, 104) = 4.087; $p = 0.0009$), and a near significant main effect for cell cycle arrest markers (F (4, 104) = 2.248; $p = 0.068$): SASP and cell cycle arrest marker expression of rapamycin treated P301SKO and P301SWT mice were similar to respective vehicle treated mice ($p = 0.9826$–0.3244; Fig. 8A–B), except for IL1β which was reduced in rapamycin treated P301SKO mice compared to vehicle treated P301SKO mice ($p = 0.0313$). SAβ-gal staining on brain cryosections of rapamycin treated transgenic mice showed an increase in β-gal activity compared to vehicle treated transgenic mice in both the presence and absence of Nrf2 (Fig. 8C). Because

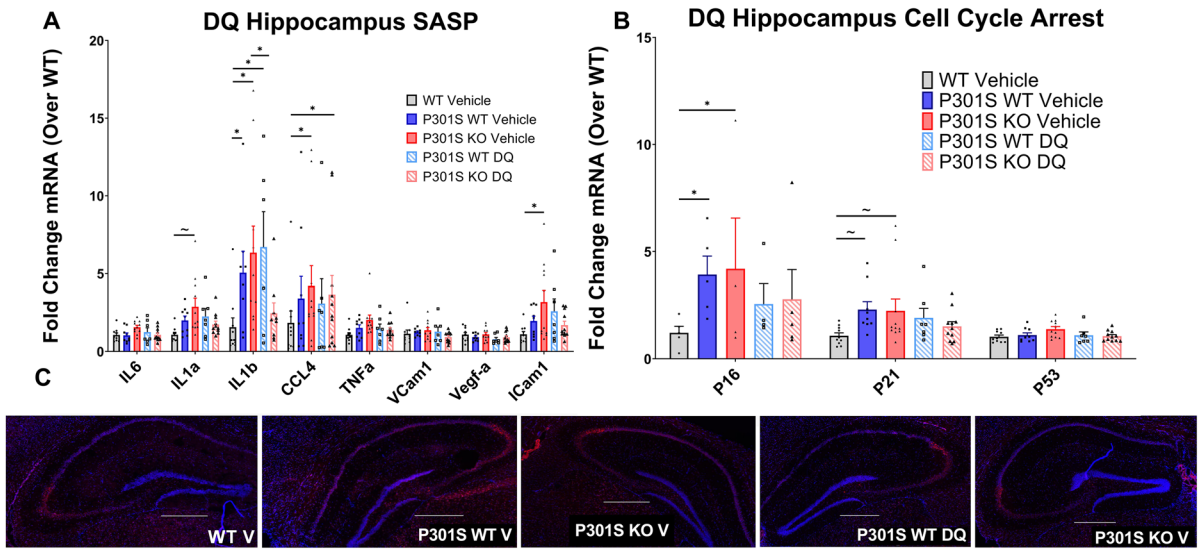

Fig. 7 DQ treatment did not reduce markers of senescence in the hippocampus of P301S mice. Senescent burden was determined by analysis of 3 biomarkers: SASP, cell cycle arrest, and SAβ-gal activity. qPCR analysis of SASP (**A**) and cell cycle arrest markers (**B**) mRNA expression in hippocampus tissue of WT vehicle (white bars), P301SWT Vehicle (gray bars), P301SKO vehicle (black bars), P301SWT DQ (striped gray bars), and P301SKO DQ (striped black bars) mice at 8.5 months of age. Analysis of Saβ-gal activity (**C**), indicated by red fluorescence (total cell number, indicated by blue fluorescence), in brain cryo-sections from WT, P301SWT, or P301SKO mice (scale bar = 500 µm. $*p < 0.05, \sim p < 0.06$ for differences between genotype defined by Fishers LSD post hoc test on a significant effect of genotype, one-way ANOVA with multiple comparisons, $n = 8$–11 per group at 8.5 months of age, data = means ± SEM)

mTOR is a repressor of the lysosomal pathway [68, 69], decreased mTOR activity resulting from rapamycin treatment likely contributes to lysosomal expansion, observed as increased SAβ-gal activity. Further analysis of isolated astrocytes, prefrontal cortex, and adipose tissue showed no significant differences in senescent marker expression between drug and vehicle treated P301SWT or P301SKO mice (Supplementary Fig. 1 a-j).

Discussion

The P301S mouse model overexpresses phosphorylation-prone 4R isoforms of human tau at fivefold higher levels than endogenous murine tau in the central nervous system, leading to neuronal loss and brain atrophy that involves hippocampus and neocortex. Neurofibrillary tangle-like inclusions develop in these regions as well as in brain stem and spinal cord, leading to severe hind-limb ataxia, paralysis, an inability to feed, and death at 9 months of age due to seeding of tau in the spinal cord [52]. It was recently reported that P301S develop senescence and cognitive impairment at 6 months of age [6], followed by severe hind limb atrophy at 9 months of age [6, 52]. Environmental factors can strongly modify the development of AD-like phenotypes in mouse models of AD, leading to substantial differences in the timing of emergence of AD-like deficits at different research facilities [70, 71]. It is currently unknown whether this is driven by differences in diet, genetic shift, or other factors. Our previous studies where we measured the ability of various mouse models of AD to model brain cellular senescence of human disease showed that cognition was not impaired at 6.5 months in the P301S model and that the onset of senescent cell accumulation was delayed until 10 months of age [15]. Consistent with these prior findings, the present studies did not demonstrate cognitive decline or senescence at 8.5 months of age for P301SWT mice. Further, we found that the onset of hind-limb paralysis was delayed to 13 months of age. It is worth considering that these delays in cognitive and motor phenotypes coincide with an absence of cellular senescence in brain, indicating a potential for senescence to be a

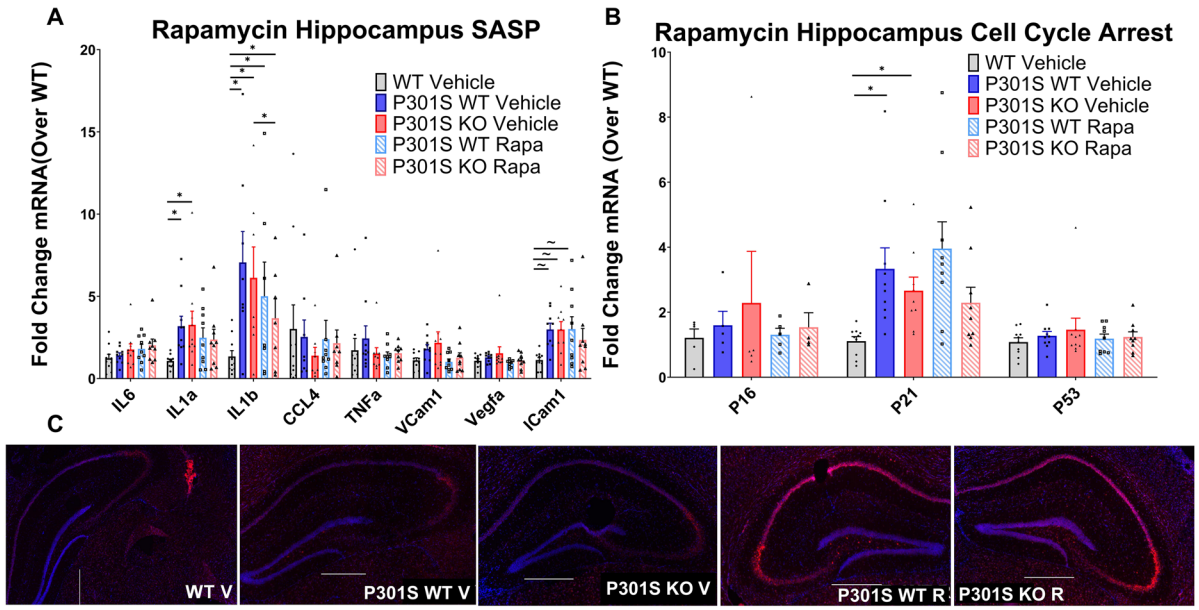

Fig. 8 Rapamycin treatment did not reduce markers of senescence in the hippocampus of P301S mice. Senescent burden was determined by analysis of 3 biomarkers: SASP, cell cycle arrest, and SAβ-gal activity. qPCR analysis of SASP (**A**) and cell cycle arrest markers (**B**) mRNA expression in hippocampus tissue of WT Vehicle (white bars), P301SWT vehicle (gray bars), P301SKO vehicle (black bars), P301SWT rapamycin (striped gray bars), and P301SKO rapamycin (striped black bars) mice at 8.5 months of age. Analysis of Saβ-gal activity (**C**), indicated by red fluorescence (total cell number, indicated by blue fluorescence), in brain cryo-sections from WT, P301SWT, or P301SKO mice (scale bar = 500 μm; $*p < 0.05, \sim p < 0.06$ for differences between genotype defined by Fishers LSD post hoc test on a significant effect of genotype, one-way ANOVA with multiple comparisons, $n = 8$–11 per group at 8.5 months of age, data = means ± SEM)

factor in phenotypic variability of AD mouse models. However, significant progress needs to be made in our understanding of AD mouse models and senescence to establish this potential causal relationship.

In our colony, P301S mice express tau at 12-fold higher levels than endogenous murine tau, and develop hind-limb phenotype at 13 months of age. Genetic ablation of Nrf2 in P301S mice accelerated the hind-limb paralysis phenotype of this model from 13 months of age to 10 months of age, but contrary to hind-limb ataxia, loss of Nrf2 did not further increase brain levels of tau or pTau in P301SKO mice compared to the P301SWT group, indicating that accumulation of pTau in brain was not the trigger for hind-limb paralysis acceleration. It is possible that this discrepancy is due to the robust immunosurveillance mechanisms of the brain [72] as compared to the spinal cord. It is known that the spinal cord is highly sensitive to damage from oxidative stress compared to other tissues [73]; thus, depletion of Nrf2 may increase seeding of tau in the spinal cord and exacerbate the phenotype.

At 8.5 months of age, P301SWT mice did not exhibit long-term memory impairment or decline in cognitive flexibility in the MWM. However, in the absence of Nrf2, P301SKO mice performed mildly but significantly worse than WT mice in tests of memory of platform location, indicating that loss of Nrf2 may have accelerated cognitive decline. At 8.5 months of age, P301SWT and P301SKO mice did not show evidence of senescent cell accumulation. While elimination of Nrf2 mildly impaired cognitive performance, it did not rely on increased senescent cell burden to do so. These data suggest that the cognitive and physical impacts of Nrf2 depletion in tau pathology are not dependent on cellular senescence as a mechanism. However, we did not measure senescent burden in spinal cord. It is thus possible that this region was more sensitive to loss of Nrf2, resulting in increased senescent cell burden that could be associated with hind-limb ataxia. Although cellular senescence was the focus of this study, a different group has shown that Nf2KO mice exhibit cognitive decline

at 20 months of age as a result of mitochondrial dysfunction and increased synaptic dysfunction [67]. It may thus be possible that the impact of Nrf2 ablation on cognition and synaptic function relies on effects of mitochondrial dysfunction unrelated to senescent cell burden.

Lastly, a more detailed investigation on the onset of senescent cell burden in our model is needed. In our hands, P301S mice develop cellular senescence in the hippocampus at 10 months of age, before emergence of hind-limb ataxia [15]. It is possible that Nrf2 deficient mice may develop elevated levels of senescence in the brain after 8.5 months of age, but before the onset of hind-limb ataxia at 10 months of age. Since we observed a significant acceleration of hind-limb and cognitive phenotypes without an increase in senescent burden in the brain, either another tissue may play a role, or another cellular pathway may be responsible for these impairments.

DQ has been shown to eliminate senescence of aged mice in multiple tissues, including the brain, alleviating brain inflammation, bone loss, and physical dysfunction [10, 74, 75]. DQ treatment also alleviated NFT burden in a mouse model of tauopathy, although it was unclear whether DQ treatment had effectively cleared senescent cells in brain [76]. In the present study, long-term DQ treatment was unable to improve cognitive performance or reduce senescent burden in brains of P301S mice independent of Nrf2 status. This may be attributed to the lack of senescent cell accumulation in brains of P301S mice at this age, or alternatively, DQ might be ineffective at eliminating senescent cells from the brain of this model. It has been noted that senescence is not a homogenous event, in that senescent cells from different inducers, cell types, and animal models produce unique SASP profiles as well as senescent cell anti-apoptotic pathways (SCAPs) [18]. While DQ has been shown to remove senescent cells from brains of aged mice by targeting SCAP proteins [10, 12, 57, 75, 77], it has not been shown to impact senescence in brains of mouse models of AD, had not previously been tested in the P301S or Nrf2KO models, and may not be the ideal senolytic treatment for P301S mice or senescence induced by Nrf2 ablation. Perhaps another senolytic such as ABT-263 or navitoclax might be more effective for this study [6, 17].

Rapamycin prevents senescent cell accumulation in different cell types and from multiple senescence inducers [28–30]. Numerous studies indicate that rapamycin reduces amyloid plaque burden and improves cognition in the hAPP(J20) [31–33, 78], P301S(PS19) [34], 3XTg-AD [25, 61, 79], and viral vector-based P301L [35] mouse models of AD and tauopathy. Previous work in our lab showed that rapamycin can prevent but not clear senescent accumulation in mouse embryonic fibroblasts as well as in the lung and adipose tissue of mice through an Nrf2 dependent manner [27]. In the present study, long-term treatment with rapamycin delayed spatial learning and led to a modest decrease in spatial memory. It is important to note that the dose that was used in our studies is fourfold higher than the dose that was used in prior studies in AD models and it is currently unknown if rapamycin administered by I.P. injection crosses the blood–brain barrier to the same extent that drug administered orally by supplementation in the chow [25, 31, 33, 61, 78, 79]. If rapamycin administered via I.P. did not effectively cross the blood brain barrier, that may explain why we did not observe equal or improved cognitive performance as compared to vehicle treated mice, although spatial learning and memory in this group were indistinguishable from that of WT littermate mice. However, we did not find that rapamycin reduced senescence markers in peripheral tissue. AD mouse models also tend to be sensitive to mouse handling, so frequent I.P. injection could have possibly been a confounding factor for our results, although both rapamycin and vehicle treatments were performed by I.P. injection. Apart from being able to extend health and lifespan in various animal models, rapamycin treatment can conversely cause metabolic disorders including vascular and mitochondrial dysfunction if given at too high of a dose or for too long [80]. Because we treated our experimental groups with doses higher than those used in other prior studies in models of AD, it is possible that we have engaged some of these detrimental mechanisms although other studies using higher doses of rapamycin have shown substantial beneficial effects in a variety of models of aging and age-associated disease [59]. Taking this in consideration with the fact that rapamycin alleviates AD-like cognitive and histopathological deficits both before [32] or after disease onset [31, 33] or in other models only pre-symptomatically [79], and termination of rapamycin treatment can result in the

relapse of cancers [81], the use of rapamycin for AD and other dementias will likely require careful determination of adequate doses.

Ultimately, in this study, we found that elimination of Nrf2 could accelerate the progression of cognitive decline in a tau-based AD model. Previous studies reported that crossing mouse models of AD featuring amyloid pathology with Nrf2KO mice results in advanced disease phenotypes [1, 47, 51, 53, 54], but had not assessed its potential impact on models of tauopathy. Despite coinciding evidence that increased levels of senescence [76, 82–84] and decreased levels of Nrf2 [46–48] are features observed in the brains of AD patients, the connection between Nrf2 and senescence in AD development has yet to be fully explored. Our results indicate that Nrf2 depletion affects tau pathology similarly to its previously described impact on amyloid pathology. However, as cognition was impaired before accumulation of senescent burden, this impairment does not appear to be dependent on cellular senescence as a mechanism. We found that a lack of cellular senescence coincided with a delay in phenotype development in P301S mice, indicating that cellular senescence may be a mechanism subject to phenotypic drift between mice raised at different animal facilities. Recently, a hypothesis emerged which predicts that rather than senescence driving plaque and tangle formation in AD, senescence acts as an external mechanism for hyperphosphorylated tau and NFTs to promote neurotoxicity [76]. In postmortem human and mouse brains, it was reported that some markers of senescence are found surrounding neurons containing NFTs, but not in neurons near depositions of Aβ plaques [7, 76]. Our data, which showed that a lack of senescence was associated with a delay in cognitive phenotype and that senescence was not the mechanism through which Nrf2 loss accelerated cognitive decline, suggests that the emergence of senescence may be causally associated with onset of cognitive decline in the P301S model, and indicate that Nrf2 protects brain function through mechanisms that may include but not require the inhibition of senescence.

Funding These studies were supported by NIH/NIA R01AG057964 to VP and VG. RR was supported by an NIH Diversity Supplement NIH/NIA R01AG057964.

Data availability Any methods, additional references, Nature Research reporting summaries, source data, statements of data availability and associated accession codes are available at https://doi.org/10.1007/s11357-023-00760-2.

Declarations

Disclaimer The content is solely the responsibility of the authors and does not necessarily represent the official views of the NIH.

Conflict of interest The authors declare no competing interests.

References

1. Rojo AI, Pajares M, García-Yagüe AJ, Buendia I, Van Leuven F, Yamamoto M, López MG, Cuadrado A. Deficiency in the transcription factor NRF2 worsens inflammatory parameters in a mouse model with combined tauopathy and amyloidopathy. Redox Biol. 2018;18:173–80. https://doi.org/10.1016/J.REDOX.2018.07.006.
2. Cao H, Wang L, Chen B, Zheng P, He Y, Ding Y, Deng Y, Lu X, Guo X, Zhang Y, Li Y, Yu G. DNA demethylation upregulated Nrf2 expression in Alzheimer's disease cellular model. Front Aging Neurosci. 2016;7:1–8. https://doi.org/10.3389/fnagi.2015.00244.
3. alzheimers-facts-and-figures.pdf (n.d.) https://www.alz.org/media/Documents/alzheimers-facts-and-figures.pdf. Accessed 22 June 2022.
4. Ader I, Pénicaud L, Andrieu S, Beard JR, Davezac N, Dray C, Fazilleau N, Gourdy P, Guyonnet S, Liblau R, Parini A, Payoux P, Rampon C, Raymond-Letron I, Rolland Y, Barreto P de S, Valet P, Vergnolle N, Sierra F, Vellas B, Casteilla L. Healthy aging biomarkers: the INSPIRE's contribution, Frailty. Aging. 2021;10:313–9.
5. Campisi J, Andersen JK, Kapahi P, Melov S. Cellular senescence: a link between cancer and age-related degenerative disease? Semin Cancer Biol. 2011;21:354–9. https://doi.org/10.1016/j.semcancer.2011.09.001.
6. Bussian TJ, Aziz A, Meyer CF, Swenson BL, Van Deursen JM, Baker DJ. Clearance of senescent glial cells prevents tau-dependent pathology and cognitive decline. Nature. 2018. https://doi.org/10.1038/s41586-018-0543-y.
7. Liu R-M. Aging, cellular senescence, and Alzheimer's disease. Int J Mol Sci. 2022;23:1989. https://doi.org/10.3390/ijms23041989.
8. Coppé J-P, Desprez P-Y, Krtolica A, Campisi J. The senescence-associated secretory phenotype: the dark side of tumor suppression. Annu Rev Pathol. 2010;5:99–118. https://doi.org/10.1146/annurev-pathol-121808-102144.
9. Cevenini E, Monti D, Franceschi C. Inflamm-ageing. Curr Opin Clin Nutr Metab Care. 2013;16:14–20. https://doi.org/10.1097/MCO.0b013e32835ada13.
10. Ogrodnik M, Evans SA, Fielder E, Victorelli S, Kruger P, Salmonowicz H, Weigand BM, Patel AD, Pirtskhalava T, Inman CL, Johnson KO, Dickinson SL, Rocha A, Schafer MJ, Zhu Y, Allison DB, von Zglinicki T,

LeBrasseur NK, Tchkonia T, Neretti N, Passos JF, Kirkland JL, Jurk D. Whole-body senescent cell clearance alleviates age-related brain inflammation and cognitive impairment in mice. Aging Cell. 2021;20. https://doi.org/10.1111/acel.13296.
11. Baker DJ, Childs BG, Durik M, Wijers ME, Sieben CJ, Zhong J, Saltness RA, Jeganathan KB, Verzosa GC, Pezeshki A, Khazaie K, Miller JD, Van Deursen JM. Naturally occurring p16 Ink4a-positive cells shorten healthy lifespan. Nature. 2016. https://doi.org/10.1038/nature16932.
12. Zhu Y, Tchkonia T, Pirtskhalava T, Gower AC, Ding H, Giorgadze N, Palmer AK, Ikeno Y, Hubbard GB, Lenburg M, O'Hara SP, LaRusso NF, Miller JD, Roos CM, Verzosa GC, LeBrasseur NK, Wren JD, Farr JN, Khosla S, Stout MB, McGowan SJ, Fuhrmann-Stroissnigg H, Gurkar AU, Zhao J, Colangelo D, Dorronsoro A, Ling YY, Barghouthy AS, Navarro DC, Sano T, Robbins PD, Niedernhofer LJ, Kirkland JL. The Achilles' heel of senescent cells: from transcriptome to senolytic drugs. Aging Cell. 2015;14:644–58. https://doi.org/10.1111/acel.12344.
13. Baker DJ, Wijshake T, Tchkonia T, LeBrasseur NK, Childs BG, van de Sluis B, Kirkland JL, van Deursen JM. Clearance of p16Ink4a-positive senescent cells delays ageing-associated disorders. Nature. 2011;479:232–6. https://doi.org/10.1038/nature10600.
14. Coppé J-P, Patil CK, Rodier F, Sun Y, Muñoz DP, Goldstein J, Nelson PS, Desprez P-Y, Campisi J. Senescence-associated secretory phenotypes reveal cell-nonautonomous functions of oncogenic RAS and the p53 tumor suppressor. PLoS Biol. 2008;6:2853–68. https://doi.org/10.1371/journal.pbio.0060301.
15. Dorigatti AO, Riordan R, Yu Z, Ross G, Wang R, Reynolds-Lallement N, Magnusson K, Galvan V, Perez VI. Brain cellular senescence in mouse models of Alzheimer's disease. GeroScience. 2022;44:1157–68. https://doi.org/10.1007/s11357-022-00531-5.
16. Bhat R, Crowe EP, Bitto A, Moh M, Katsetos CD, Garcia FU, Johnson FB, Trojanowski JQ, Sell C, Torres C. Astrocyte senescence as a component of Alzheimer's disease. PLoS ONE. 2012;7:e45069–e45069. https://doi.org/10.1371/journal.pone.0045069.
17. Zhu Y, Tchkonia T, Fuhrmann-Stroissnigg H, Dai HM, Ling YY, Stout MB, Pirtskhalava T, Giorgadze N, Johnson KO, Giles CB, Wren JD, Niedernhofer LJ, Robbins PD, Kirkland JL. Identification of a novel senolytic agent, navitoclax, targeting the Bcl-2 family of anti-apoptotic factors. Aging Cell. 2016;15:428–35. https://doi.org/10.1111/acel.12445.
18. Niedernhofer LJ, Robbins PD. Senotherapeutics for healthy ageing. Nat Rev Drug Discov. 2018;17:377–377. https://doi.org/10.1038/nrd.2018.44.
19. McCormick MA, Tsai S-Y, Kennedy BK. TOR and ageing: a complex pathway for a complex process. Philos Trans R Soc Lond B Biol Sci. 2011;366:17–27. https://doi.org/10.1098/rstb.2010.0198.
20. Harrison DE, Strong R, Sharp ZD, Nelson JF, Astle CM, Flurkey K, Nadon NL, Wilkinson JE, Frenkel K, Carter CS, Pahor M, Javors MA, Fernandez E, Miller RA. Rapamycin fed late in life extends lifespan in genetically heterogeneous mice. Nature. 2009;460:392–5. https://doi.org/10.1038/nature08221.
21. Wilkinson JE, Burmeister L, Brooks SV, Chan C-C, Friedline S, Harrison DE, Hejtmancik JF, Nadon N, Strong R, Wood LK, Woodward MA, Miller RA. Rapamycin slows aging in mice. Aging Cell. 2012;11:675–82. https://doi.org/10.1111/j.1474-9726.2012.00832.x.
22. Miller RA, Harrison DE, Astle CM, Baur JA, Boyd AR, de Cabo R, Fernandez E, Flurkey K, Javors MA, Nelson JF, Orihuela CJ, Pletcher S, Sharp ZD, Sinclair D, Starnes JW, Wilkinson JE, Nadon NL, Strong R. Rapamycin, but not resveratrol or simvastatin, extends life span of genetically heterogeneous mice. J Gerontol A Biol Sci Med Sci. 2011;66:191–201. https://doi.org/10.1093/gerona/glq178.
23. Van Skike CE, Lin A-L, Roberts Burbank R, Halloran JJ, Hernandez SF, Cuvillier J, Soto VY, Hussong SA, Jahrling JB, Javors MA, Hart MJ, Fischer KE, Austad SN, Galvan V. mTOR drives cerebrovascular, synaptic, and cognitive dysfunction in normative aging. Aging Cell. 2020;19:e13057. https://doi.org/10.1111/acel.13057.
24. Halloran J, Hussong SA, Burbank R, Podlutskaya N, Fischer KE, Sloane LB, Austad SN, Strong R, Richardson A, Hart MJ, Galvan V. Chronic inhibition of mammalian target of rapamycin by rapamycin modulates cognitive and non-cognitive components of behavior throughout lifespan in mice. Neuroscience. 2012;223:102–13. https://doi.org/10.1016/j.neuroscience.2012.06.054.
25. Caccamo A, De Pinto V, Messina A, Branca C, Oddo S. Genetic reduction of mammalian target of rapamycin ameliorates Alzheimer's disease-like cognitive and pathological deficits by restoring hippocampal gene expression signature. J Neurosci Off J Soc Neurosci. 2014;34:7988–98. https://doi.org/10.1523/JNEUROSCI.0777-14.2014.
26. Johnson SC, Sangesland M, Kaeberlein M, Rabinovitch PS. Modulating mTOR in aging and health. Interdiscip Top Gerontol. 2015;40:107–27. https://doi.org/10.1159/000364974.
27. Wang R, Yu Z, Sunchu B, Shoaf J, Dang I, Zhao S, Caples K, Bradley L, Beaver LM, Ho E, Löhr CV, Perez VI. Rapamycin inhibits the secretory phenotype of senescent cells by a Nrf2-independent mechanism. Aging Cell. 2017;16:564–74. https://doi.org/10.1111/acel.12587.
28. Demidenko ZN, Zubova SG, Bukreeva EI, Pospelov VA, Pospelova TV, Blagosklonny MV. Rapamycin decelerates cellular senescence. Cell Cycle Georget Tex. 2009;8:1888–95. https://doi.org/10.4161/cc.8.12.8606.
29. Cao K, Graziotto JJ, Blair CD, Mazzulli JR, Erdos MR, Krainc D, Collins FS. Rapamycin reverses cellular phenotypes and enhances mutant protein clearance in Hutchinson-Gilford progeria syndrome cells. Sci Transl Med. 2011;3:89ra58. https://doi.org/10.1126/scitranslmed.3002346.
30. Iglesias-Bartolome R, Patel V, Cotrim A, Leelahavanichkul K, Molinolo AA, Mitchell JB, Gutkind JS. mTOR inhibition prevents epithelial stem cell senescence and protects from radiation-induced mucositis. Cell Stem Cell. 2012;11:401–14. https://doi.org/10.1016/j.stem.2012.06.007.
31. Lin A-L, Zheng W, Halloran JJ, Burbank RR, Hussong SA, Hart MJ, Javors M, Shih Y-YI, Muir E, Solano Fonseca R, Strong R, Richardson AG, Lechleiter JD, Fox PT, Galvan V. Chronic rapamycin restores brain vascular integrity and function through NO synthase activation

and improves memory in symptomatic mice modeling Alzheimer's disease. J Cereb Blood Flow Metab Off J Int Soc Cereb Blood Flow Metab. 2013;33:1412–21. https://doi.org/10.1038/jcbfm.2013.82.
32. Spilman P, Podlutskaya N, Hart MJ, Debnath J, Gorostiza O, Bredesen D, Richardson A, Strong R, Galvan V. Inhibition of mTOR by rapamycin abolishes cognitive deficits and reduces amyloid-β levels in a mouse model of alzheimer's disease. PLoS ONE. 2010;5:e9979–e9979. https://doi.org/10.1371/journal.pone.0009979.
33. Van Skike CE, Hussong SA, Hernandez SF, Banh AQ, DeRosa N, Galvan V. mTOR attenuation with rapamycin reverses neurovascular uncoupling and memory deficits in mice modeling Alzheimer's disease. J Neurosci. 2021;41:4305–20. https://doi.org/10.1523/JNEUROSCI.2144-20.2021.
34. Ozcelik S, Fraser G, Castets P, Schaeffer V, Skachokova Z, Breu K, Clavaguera F, Sinnreich M, Kappos L, Goedert M, Tolnay M, Winkler DT. Rapamycin attenuates the progression of tau pathology in P301S tau transgenic mice. PloS One. 2013;8:e62459. https://doi.org/10.1371/journal.pone.0062459.
35. Siman R, Cocca R, Dong Y. The mTOR inhibitor rapamycin mitigates perforant pathway neurodegeneration and synapse loss in a mouse model of early-stage Alzheimer-type tauopathy. PloS One. 2015;10:e0142340. https://doi.org/10.1371/journal.pone.0142340.
36. Wang Z, Chen Z, Jiang Z, Luo P, Liu L, Huang Y, Wang H, Wang Y, Long L, Tan X, Liu D, Jin T, Wang Y, Wang Y, Liao F, Zhang C, Chen L, Gan Y, Liu Y, Yang F, Huang C, Miao H, Chen J, Cheng T, Fu X, Shi C. Cordycepin prevents radiation ulcer by inhibiting cell senescence via NRF2 and AMPK in rodents. Nat Commun. 2018. https://doi.org/10.1038/s41467-019-10386-8.
37. Wang Z, Wang L, Jiang R, Li C, Chen X, Xiao H, Hou J, Hu L, Huang C, Wang Y. Ginsenoside Rg1 prevents bone marrow mesenchymal stem cell senescence via NRF2 and PI3K/Akt signaling. Free Radic Biol Med. 2021;174:182–94. https://doi.org/10.1016/j.freeradbiomed.2021.08.007.
38. Kapeta S, Chondrogianni N, Gonos ES. Nuclear erythroid factor 2-mediated proteasome activation delays senescence in human fibroblasts*. J Biol Chem. 2010;285:8171–84. https://doi.org/10.1074/jbc.M109.031575.
39. Chan Y-C, Lee I-T, Wang M-F, Yeh W-C, Liang B-C. Tempeh attenuates cognitive deficit, antioxidant imbalance, and amyloid β of senescence-accelerated mice by modulating Nrf2 expression via MAPK pathway. J Funct Foods. 2018;50:112–9. https://doi.org/10.1016/j.jff.2018.09.023.
40. Romero A, Hipólito-Luengo Álvaro S, Villalobos LA, Vallejo S, Valencia I, Michalska P, Pajuelo-Lozano N, Sánchez-Pérez I, Rafael León J, Bartha Luis, María J, Sanz J.D. Erusalimsky, Sánchez-Ferrer Carlos F, Romacho T, Peiró Concepción. The angiotensin-(1–7)/Mas receptor axis protects from endothelial cell senescence via klotho and Nrf2 activation. Aging Cell. 2019;18:12913. https://doi.org/10.1111/acel.12913.
41. Sanjay S, Girish C, Toi PC, Bobby Z. Quercetin modulates NRF2 and NF-κB/TLR-4 pathways to protect against isoniazid- and rifampicin-induced hepatotoxicity in vivo. Can J Physiol Pharmacol. 2021;99:952–63. https://doi.org/10.1139/cjpp-2021-0008.
42 De Prax MCA, Ferro KPV, Santos I, Torello CO, Salazar-Terreros M, Olalla Saad ST. NRF2 is targeted by the polyphenol quercetin and induces apoptosis, in part, through up regulation of pro apoptotic miRs. Blood. 2019;134:2529. https://doi.org/10.1182/blood-2019-130982.
43. Sykiotis GP, Bohmann D. Keap1/Nrf2 signaling regulates oxidative stress tolerance and lifespan in Drosophila. Dev Cell. 2008;14:76–85. https://doi.org/10.1016/j.devcel.2007.12.002.
44. Smith EJ, Shay KP, Thomas NO, Butler JA, Finlay LF, Hagen TM. Age-related loss of hepatic Nrf2 protein homeostasis: potential role for heightened expression of miR-146a. Free Radic Biol Med. 2015;89:1184–91. https://doi.org/10.1016/j.freeradbiomed.2015.11.003.
45 Hayes JD, Dinkova-Kostova AT. The Nrf2 regulatory network provides an interface between redox and intermediary metabolism. Trends Biochem Sci. 2014;39(4):199–218. https://doi.org/10.1016/j.tibs.2014.02.002.
46. Ramsey CP, Glass CA, Montgomery MB, Lindl KA, et al. Expression of Nrf2 in neurodegenerative diseases. J Neuropathol Exp Neurol. 2007;66:75–85.
47. Rojo AI, Pajares M, Rada P, Nuñez A, Nevado-Holgado AJ, Killik R, Leuven FV, Ribe E, Lovestone S, Yamamoto M, Cuadrado A. NRF2 deficiency replicates transcriptomic changes in Alzheimer's patients and worsens APP and TAU pathology. Redox Biol. 2017;13:444–51. https://doi.org/10.1016/j.redox.2017.07.006.
48. Yang Y, Jiang S, Yan J, Li Y, Xin Z, Lin Y, Qu Y. An overview of the molecular mechanisms and novel roles of Nrf2 in neurodegenerative disorders. Cytokine Growth Factor Rev. 2015;26:47–57. https://doi.org/10.1016/j.cytogfr.2014.09.002.
49. Volonte D, Liu Z, Musille PM, Stoppani E, Wakabayashi N, Di Y-P, Lisanti MP, Kensler TW, Galbiati F. Inhibition of nuclear factor-erythroid 2–related factor (Nrf2) by caveolin-1 promotes stress-induced premature senescence. Mol Biol Cell. 2013;24:1852–62. https://doi.org/10.1091/mbc.e12-09-0666.
50. Tarantini S, Valcarcel-Ares MN, Yabluchanskiy A, Tucsek Z, Hertelendy P, Kiss T, Gautam T, Zhang XA, Sonntag WE, de Cabo R, Farkas E, Elliott MH, Kinter MT, Deak F, Ungvari Z, Csiszar A. Nrf2 deficiency exacerbates obesity-induced oxidative stress, neurovascular dysfunction, blood–brain barrier disruption, neuroinflammation, amyloidogenic gene expression, and cognitive decline in mice, mimicking the aging phenotype. J Gerontol A Biol Sci Med Sci. 2018;73:853–63. https://doi.org/10.1093/gerona/glx177.
51. Joshi G, Ann Gan K, Johnson DA, Johnson JA. Increased Alzheimer's disease-like pathology in the APP/ PS1ΔE9 mouse model lacking Nrf2 through modulation of autophagy. Neurobiol Aging. 2015;36:664–79. https://doi.org/10.1016/j.neurobiolaging.2014.09.004.
52. Yoshiyama Y, Higuchi M, Zhang B, Huang S-M, Iwata N, Saido TC, Maeda J, Suhara T, Trojanowski JQ, Lee VM-Y. Synapse loss and microglial activation precede tangles in a P301S tauopathy mouse model. Neuron.

2007;53:337–51. https://doi.org/10.1016/j.neuron.2007.01.010.
53. Ren P, Chen J, Li B, Zhang M, Yang B, Guo X, Chen Z, Cheng H, Wang P, Wang S, Wang N, Zhang G, Wu X, Ma D, Guan D, Zhao R. Nrf2 ablation promotes Alzheimer's disease-like pathology in APP/PS1 transgenic mice: the role of neuroinflammation and oxidative stress. Oxid Med Cell Longev. 2020;2020:e3050971. https://doi.org/10.1155/2020/3050971.
54. Branca C, Ferreira E, Nguyen T-V, Doyle K, Caccamo A, Oddo S. Genetic reduction of Nrf2 exacerbates cognitive deficits in a mouse model of Alzheimer's disease. Hum Mol Genet. 2017;26:4823–35. https://doi.org/10.1093/hmg/ddx361.
55. Raffaele M, Kovacovicova K, Frohlich J, Re OL, Giallongo S, Oben JA, Faldyna M, Leva L, Giannone AG, Cabibi D, Vinciguerra M. Mild exacerbation of obesity- and age-dependent liver disease progression by senolytic cocktail dasatinib + quercetin. Cell Commun Signal. 2021;19:1–9 (http://dx.doi.org.ezproxy.proxy.library.oregonstate.edu/10.1186/s12964-021-00731-0).
56. Ogrodnik M, Zhu Y, Langhi LGP, Tchkonia T, Krüger P, Fielder E, Victorelli S, Ruswhandi RA, Giorgadze N, Pirtskhalava T, Podgorni O, Enikolopov G, Johnson KO, Xu M, Inman C, Schafer M, Weigl M, Ikeno Y, Burns TC, Passos JF, von Zglinicki T, Kirkland JL, Jurk D. Obesity-induced cellular senescence drives anxiety and impairs neurogenesis. Cell Metab. 2019. https://doi.org/10.1016/j.cmet.2018.12.008.
57. Saccon TD, Nagpal R, Yadav H, Cavalcante MB, Nunes AD de C, Schneider A, Gesing A, Hughes B, Yousefzadeh M, Tchkonia T, Kirkland JL, Niedernhofer LJ, Robbins PD, Masternak MM. Senolytic Combination of dasatinib and quercetin alleviates intestinal senescence and inflammation and modulates the gut microbiome in aged mice. J Gerontol A Biol Sci Med Sci. 2021;76:1895–905. https://doi.org/10.1093/gerona/glab002.
58. Palmer AK, Xu M, Zhu Y, Pirtskhalava T, Weivoda MM, Hachfeld CM, Prata LG, van Dijk TH, Verkade E, Casaclang-Verzosa G, Johnson KO, Cubro H, Doornebal EJ, Ogrodnik M, Jurk D, Jensen MD, Chini EN, Miller JD, Matveyenko A, Stout MB, Schafer MJ, White TA, Hickson LJ, Demaria M, Garovic V, Grande J, Arriaga EA, Kuipers F, von Zglinicki T, LeBrasseur NK, Campisi J, Tchkonia T, Kirkland JL. Targeting senescent cells alleviates obesity-induced metabolic dysfunction. Aging Cell. 2019;18:e12950. https://doi.org/10.1111/acel.12950.
59. Bitto A, Ito TK, Pineda VV, LeTexier NJ, Huang HZ, Sutlief E, Tung H, Vizzini N, Chen B, Smith K, Meza D, Yajima M, Beyer RP, Kerr KF, Davis DJ, Gillespie CH, Snyder JM, Treuting PM, Kaeberlein M. Transient rapamycin treatment can increase lifespan and healthspan in middle-aged mice. ELife. 2016;5:e16351. https://doi.org/10.7554/eLife.16351.
60. Ramos FJ, Chen SC, Garelick MG, Dai D-F, Liao C-Y, Schreiber KH, MacKay VL, An EH, Strong R, Ladiges WC, Rabinovitch PS, Kaeberlein M, Kennedy BK. Rapamycin reverses elevated mTORC1 signaling in lamin A/C-deficient mice, rescues cardiac and skeletal muscle function, and extends survival. Sci Transl Med. 2012;4:144ra103. https://doi.org/10.1126/scitranslmed.3003802.
61. Caccamo A, Majumder S, Richardson A, Strong R, Oddo S. Molecular interplay between mammalian target of rapamycin (mTOR), amyloid-beta, and Tau: effects on cognitive impairments. J Biol Chem. 2010;285:13107–20. https://doi.org/10.1074/jbc.M110.100420.
62. Van Skike CE, Galvan V. A Perfect sTORm: The role of the mammalian target of rapamycin (mTOR) in cerebrovascular dysfunction of Alzheimer's disease: a mini-review. Gerontology. 2018;64:205–11. https://doi.org/10.1159/000485381.
63. Zamzow DR, Elias V, Acosta VA, Escobedo E, Magnusson KR. Higher levels of phosphorylated Y1472 on GluN2B subunits in the frontal cortex of aged mice are associated with good spatial reference memory, but not cognitive flexibility. Age. 2016;38:50. https://doi.org/10.1007/s11357-016-9913-2.
64. Schimanski LA, Lipa P, Barnes CA. Tracking the course of hippocampal representations during learning: when is the map required? J Neurosci. 2013;33:3094–106. https://doi.org/10.1523/JNEUROSCI.1348-12.2013.
65. Maei HR, Zaslavsky K, Teixeira CM, Frankland PW. What is the most sensitive measure of water maze probe test performance? Front Integr Neurosci. 2009;3:4. https://doi.org/10.3389/neuro.07.004.2009.
66. Marrone DF, Ramirez-Amaya V, Barnes CA. Neurons generated in senescence maintain capacity for functional integration. Hippocampus. 2012;22:1134–42. https://doi.org/10.1002/hipo.20959.
67. Zweig JA, Caruso M, Brandes MS, Gray NE. Loss of NRF2 leads to impaired mitochondrial function, decreased synaptic density and exacerbated age-related cognitive deficits. Exp Gerontol. 2020;131:110767. https://doi.org/10.1016/j.exger.2019.110767.
68. Antikainen H, Driscoll M, Haspel G, Dobrowolski R. TOR-mediated regulation of metabolism in aging. Aging Cell. 2017;16:1219–33. https://doi.org/10.1111/acel.12689.
69. Kimura T, Hayama Y, Okuzaki D, Nada S, Okada M. The Ragulator complex serves as a substrate-specific mTORC1 scaffold in regulating the nuclear translocation of transcription factor EB. J Biol Chem. 2022;298(3):101744. https://doi.org/10.1016/j.jbc.2022.101744.
70. Jankowsky JL, Melnikova T, Fadale DJ, Xu GM, Slunt HH, Gonzales V, Younkin LH, Younkin SG, Borchelt DR, Savonenko AV. Environmental enrichment mitigates cognitive deficits in a mouse model of Alzheimer's disease. J Neurosci. 2005;25:5217–24. https://doi.org/10.1523/JNEUROSCI.5080-04.2005.
71. Sauce B, Bendrath S, Herzfeld M, Siegel D, Style C, Rab S, Korabelnikov J, Matzel LD. The impact of environmental interventions among mouse siblings on the heritability and malleability of general cognitive ability. Philos Trans R Soc B Biol Sci. 2018;373:20170289. https://doi.org/10.1098/rstb.2017.0289.
72. Stolp HB, Liddelow SA, Sá-Pereira I, Dziegielewska KM, Saunders NR. Immune responses at brain barriers and implications for brain development and neurological

function in later life. Front Integr Neurosci. 2013;7:61. https://doi.org/10.3389/fnint.2013.00061.
73. Visavadiya NP, Patel SP, VanRooyen JL, Sullivan PG, Rabchevsky AG. Cellular and subcellular oxidative stress parameters following severe spinal cord injury. Redox Biol. 2016;8:59–67. https://doi.org/10.1016/j.redox.2015.12.011.
74. Farr JN, Xu M, Weivoda MM, Monroe DG, Fraser DG, Onken JL, Negley BA, Sfeir JG, Ogrodnik MB, Hachfeld CM, LeBrasseur NK, Drake MT, Pignolo RJ, Pirtskhalava T, Tchkonia T, Oursler MJ, Kirkland JL, Khosla S. Targeting cellular senescence prevents age-related bone loss in mice. Nat Med. 2017;23:1072–9. https://doi.org/10.1038/nm.4385.
75. Xu M, Pirtskhalava T, Farr JN, Weigand BM, Palmer AK, Weivoda MM, Inman CL, Ogrodnik MB, Hachfeld CM, Fraser DG, Onken JL, Johnson KO, Verzosa GC, Langhi LGP, Weigl M, Giorgadze N, LeBrasseur NK, Miller JD, Jurk D, Singh RJ, Allison DB, Ejima K, Hubbard GB, Ikeno Y, Cubro H, Garovic VD, Hou X, Weroha SJ, Robbins PD, Niedernhofer LJ, Khosla S, Tchkonia T, Kirkland JL. Senolytics improve physical function and increase lifespan in old age. Nat Med. 2018;24:1246–56. https://doi.org/10.1038/s41591-018-0092-9.
76. Musi N, Valentine JM, Sickora KR, Baeuerle E, Thompson CS, Shen Q, Orr ME. Tau protein aggregation is associated with cellular senescence in the brain. Aging Cell. 2018;17:e12840. https://doi.org/10.1111/acel.12840.
77. Kirkland JL, Tchkonia T. Senolytic drugs: from discovery to translation. J Intern Med. 2020;288:518–36. https://doi.org/10.1111/joim.13141.
78. Lin T-J, Liang W-M, Hsiao P-W, Pradeep MS, Wei W-C, Lin H-T, Yin S-Y, Yang N-S. Rapamycin promotes mouse 4T1 tumor metastasis that can be reversed by a dendritic cell-based vaccine. PLOS ONE. 2015;10:e0138335. https://doi.org/10.1371/journal.pone.0138335.
79. Majumder S, Richardson A, Strong R, Oddo S. Inducing autophagy by rapamycin before, but not after, the formation of plaques and tangles ameliorates cognitive deficits. PLoS ONE. 2011;6:e25416. https://doi.org/10.1371/journal.pone.0025416.
80. Kim EK, Min HK, Lee S-Y, Kim D-S, Ryu J-G, Na HS, Jung KA, Choi JW, Park S-H, Cho M-L. Metformin rescues rapamycin-induced mitochondrial dysfunction and attenuates rheumatoid arthritis with metabolic syndrome. Arthritis Res Ther. 2020;22:77. https://doi.org/10.1186/s13075-020-02174-3.
81. Li J, Kim SG, Blenis J. Rapamycin: One Drug, Many Effects. Cell Metab. 2014;19:373–9. https://doi.org/10.1016/j.cmet.2014.01.001.
82. Arendt T, Holzer M, Gärtner U. Neuronal expression of cycline dependent kinase inhibitors of the INK4 family in Alzheimer's disease. J Neural Transm. 1998;105:949–60. https://doi.org/10.1007/s007020050104.
83. Arendt T, Rödel L, Gärtner U, Holzer M. Expression of the cyclin-dependent kinase inhibitor p16 in Alzheimer's disease. NeuroReport. 1996;7:3047–9. https://doi.org/10.1097/00001756-199611250-00050.
84. Lüth HJ, Holzer M, Gertz HJ, Arendt T. Aberrant expression of nNOS in pyramidal neurons in Alzheimer's disease is highly co-localized with p21ras and p16INK4a. Brain Res. 2000;852:45–55. https://doi.org/10.1016/s0006-8993(99)02178-2.